

Searching for Lepton Flavor Violation with the MEG experiment (or looking for flying pigs)

S. Dussoni^a *on behalf of the MEG collaboration.*

^aINFN and Università di Genova,
via Dodecaneso 33, 16146 Genova (Italy).

As the Standard Model encounters several philosophical problems, New Physics is expected to be found slightly above the mass scale currently probed. Effects due to non-Standard Model features can be easily tagged by the observation of Charged Lepton Flavor Violation. Thus the MEG experiment has been designed and is currently in an advanced phase having started data taking in summer 2008 and is expected to give at least an upper limit on the $\mu \rightarrow e + \gamma$ decay two order of magnitude better than the current limit[1] set by the MEGA collaboration[2]. Here all experimental challenges are shown together with the main detector features. the

1. Some theory backgrounds

The Standard Model (SM) has long been regarded as the definitive model for particle behavior, thanks mainly to its striking success in predicting experimental results. However many things remained unresolved, and many theories have been proposed to improve the SM. But all these beautiful constructions need tests in order to be rejected or validated or simply to constrain their parameter space in order to account for experimental observation and achieve a status of "predictive" theory. A very promising field to be probed in search of effects of new physics is the one of Lepton Flavor Violating processes (LFV) involving charged leptons. LFV has been already detected for neutrinos. So the doubt arise: LFV is possible in the charged lepton sector, within the SM? The answer is that LFV in the charged sector can't be induced within the framework of the SM even accounting for the ν oscillation mechanism, making it as likely to be observed as flying pigs, whereby alternative models can generate LFV processes such as $\mu \rightarrow e + \gamma$ with a detectable rate. The predictions for the branching ratio $BR_{\mu \rightarrow e \gamma}$ ranges from 10^{-11} , which is already excluded by the MEGA experiment, to fractions of 10^{-18} , outside reach of the MEG apparatus. Hence a search for charged LFV is a promising field for new physics (see [3], [4] and references

therein. Among particles undergoing LFV processes, muons are attractive because of the existence of very intense and pure muon beams. Two most viable channels are envisaged for muon LFV: the μ conversion in heavy nuclei and the $\mu \rightarrow e + \gamma$ decay. The ratio among these two possible mechanism is model-dependent: thus an accurate determination of both branching ratios or upper limits can disentangle several theoretical scenarios[5].

An interesting feature is the strong relationship between LFV and precision measurements such as Muon Anomalous Dipole and Magnetic moment, neutrino-less double beta decay and neutrino mass pattern. Moreover the eventual observation of LFV in the charged sector could provide complementary indications to the "huge accelerator discoveries", with a different approach than the use of growing powerful and complicated experiments: the precision measurements of a physical quantity with a small, dedicated detector, in a reasonable timescale!

2. Experimental Concept

The detection of the $\mu \rightarrow e + \gamma$ decay is subordinate to the observation of a positron and a photon emitted from the same particle simultaneously and, being a two-body decay, equally sharing the muon energy; having muons at rest, the

energy of each particle should be equal to $m_\mu/2$. The main problem is related to the rarity of the phenomenon searched, and is caused by the possible background events that can mimic the true $\mu \rightarrow e + \gamma$ decay leading to an erroneous interpretation of the acquired data. In order to minimize such occurrence a very precise measurement of the energy momentum and emission time of both positron and gamma is mandatory. Thus the MEG experiment has been designed with a two-body detector, with one sub-module dedicated to the gamma energy and time measurement and the other performing positron spectroscopy and time-tagging. A sketch of the MEG experiment

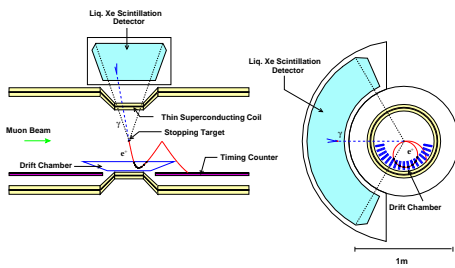


Figure 1. Schematic of the MEG experiment concept.

concept is shown in fig. 1

2.1. Liquid Xenon Calorimeter

The photon detector consists of a liquid Xenon calorimeter (LXe). This is a C-shaped vessel containing about 800 l of ultra-pure liquified Xenon, kept at a temperature of 165 K and a pressure of 3 Atm[6].

Main liquid Xenon scintillating properties[7] are a short radiation length (2.8 cm), thanks to its high $Z = 54$; a high light yield, corresponding to 75% of the standard NaI; a fast response and a large attenuation length. thanks to its peculiar light emission mechanism. Moreover it is uniform and monolithic, which improves response with respect to conventional crystals. Other VIII group

gases also show interesting scintillating properties that make them attractive for calorimetry[8]. All these characteristics match well the requirements for obtaining both a high efficiency, a good energy resolution and a timing resolution[6].

The emission mechanism[9] of Xe is due to the combination of two atoms, of which at least one in an excited state, in a bound state called “excimer”, coming from the energy deposited by particle passing through. The excimer then de-excite emitting scintillation photons and the two Xenon atoms dissociate.

The attractive feature of this process is the intrinsically null re-absorption of emitted photons, since they are emitted by an excited state of *two* bound atoms, which do not exist as a ground state. Thanks to this feature the leading edge of the Xenon emission is very steep being limited only by impurities present into the gas and by Rayleigh scattering. Both have the effect of lowering the absorption length to a value of about 40 cm. Thus it is of paramount importance to reach a very low level of contaminants in the Liquid Xenon and to maintain it during the whole operation time. A sophisticated Liquid Purification Stage has been developed for this aim[4,6].

The Xenon volume is read out with 880 PhotoMultiplier Tubes (PMT) with a quartz window and a responsivity extended to the Vacuum Ultra Violet (VUV) range, matching the Xe emission wavelength of 178 nm. Exspecial care had to be put in noise rejection as well as to obtain the best Quantum Efficiency for these devices, to pull at most the detector performances.

The final results for energy and time resolution are shown in fig. 2; they are obtained with the π_0 calibration method described in the following. It is worth noting that especially the time resolution relies in a careful reconstruction of the interaction point of the photon inside the fiducial volume, thus events occurring very near to the surface have to be rejected or analyzed with a different algorithm to account for non linearity due to PMT or electronic saturation.

2.2. Drift Chambers and COBRA magnet

These two items combined allow a precise measurement of positron momenta and trajectories

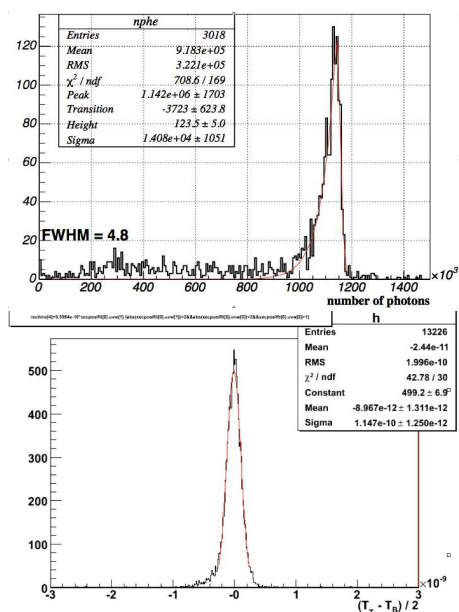


Figure 2. Upper: LXe energy resolution 5 MeV; lower: LXe timing resolution. Obtained with π_0 events.

while keeping a relatively low detector occupancy, a very important issue in limiting background events.

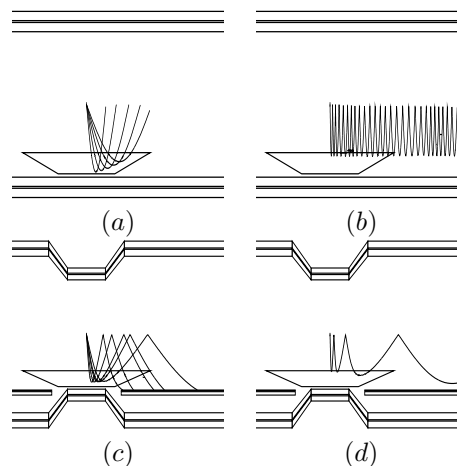


Figure 3. Problems with a *uniform solenoidal magnetic field*:

(a) Trajectories of monochromatic particles emitted at various angles. The bending radius depends on the emission angle.

(b) $r - z$ view of the solenoid shown with the trajectory of a particle emitted at 88° making many turns inside the detector.

Advantages of a *gradient magnetic field*:

(c) Trajectories of monochromatic particles emitted at various angles. The bending radius is independent of the emission angle.

(d) $r - z$ view of the COBRA spectrometer shown with the trajectory of a particle emitted at 88° . The particle is swept away more quickly than in (b).

The COBRA magnet has an inhomogeneous field designed in such a way as to provide two important features for the MEG experiment (see Figure 3).

The first one is suggested by the name COBRA, which stands for “Constant Bending Radius”: Thanks to the geometry of the magnet

coils, the field gradient is arranged in such a way that positron with equal value of momentum but with rather different directions undergo the same curvature radius, while in a conventional solenoidal field the curvature radius would be determined by the transverse momentum p_t which depends on the positron emission angle with respect to the magnet axis; so the COBRA allows for a better reconstruction of the positron momentum.

The second advantage coming from a gradient field is that positron emitted nearly perpendicular to the magnet axis are swept away from the Drift Chambers quickly, in contrast to what happens in an homogeneous field (Figure 3). The problems caused by positrons making many turns inside the Drift Chambers concern either the degradation of their performances or the loss of timing resolution due to multiple scattering inside the chambers.

The field in the COBRA magnet reaches the maximum value of 1.28 T at the center and decreases towards the spectrometer edges. The thicknesses of the winding and of the cryostat containing the whole magnet are kept as low as possible, limiting the conversion factor for a 52.8 MeV γ to about 18 %.

2.3. The Drift Chamber

The Drift Chamber will measure the energy of the outgoing positrons by recording their tracks in the magnetic field.

There are 15 trapezoidal Drift Chambers placed in a radial arrangement with an angular displacement of 17.5° ; along the COBRA axis the chambers extend from $z = -50$ cm to $z = +50$ cm (inner region) and from $z = -21.9$ cm to $z = +21.9$ cm in the outer region, thus covering a surface corresponding to the calorimeter acceptance angle. Along the radial direction, the chambers inner edge is at $r = 19.3$ cm and they extend to the inner surface of the COBRA magnet, which measures $r = 27$ cm.

Each module consists of a couple of staggered cells. The staggered-cell configuration allows for the measurement of the radial coordinates of the track. The difference between the drift times ($t_1 - t_2$) in two adjacent cells gives the r -coordinate of the track with a $\sim 150 \mu\text{m}$ accuracy,

while the mean time $(t_1 + t_2)/2$ gives the absolute time of the track with ~ 5 ns accuracy. This excellent position resolution is important for the track reconstruction, allowing for an angular resolution $\delta\theta = 0.2$ mrad. The chambers are filled with a 1:1 mixture of CH_4 and He, providing sufficient ionization while minimizing the multiple scattering which is the main limiting factor for an ultimate spatial resolution.

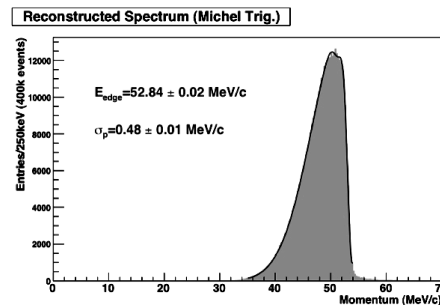


Figure 4. Drift Chamber resolution of reconstructed Michel spectrum end point.

In fig. 4 the reconstructed end point for Michel positron spectrum is shown, together with the measured energy and momentum resolution which satisfies the required values for the MEG experiment planned sensitivity.

2.4. The Timing Counter

After leaving the Drift Chambers the positrons hit the Timing Counter. The aim of the Timing Counter is to provide a fast signal from positrons in order to obtain both a very precise ($\Delta T = 100$ ps FWHM) determination of the instant in which the particle is ejected from the target and a reliable detection of positron-photon coincidence for triggering purposes.

There are two identical Timing Counter modules, placed in symmetrical position with respect to the axis origin. They are placed on the inner surface of the two outermost coils of the COBRA magnet in a position that will allow for the de-

tection of all positrons emitted within the solid angle opposite to the LXe calorimeter.

Each Timing Counter module consists in a longitudinal detector which is optimized for timing purposes, and a transverse one that is intended to provide the triggering signal for the DAQ system. The latter is located in the inner zone at a radius $r = 280$ mm while the mean radius of the longitudinal detector is 315 mm.

Each longitudinal detector is an assembly of 15 scintillator bars whose light output is read by two PMTs, one for each end. Special PMTs suitable for use in magnetic field have been selected: the best candidate proved to be the HAMAMATSU fine mesh type, and we decided to use the 2" model R5924[10], well matching the optimal shape of the scintillator bar[11]. Several beam test held at the Laboratori Nazionali di Frascati's "Beam Test Facility" (BTF) allowed us to obtain the goal resolution with an almost squared section of 4 cm, and using BC404 scintillator from Bicron Saint Gobain[12] With this geometry the matching PMT-scintillator is optimum and a timing resolution better than 100 ps FWHM has been obtained (see fig. 5).

For the transverse detector the PMT readout was found not to be possible due to the strong magnetic field in the zone of the detectors, so we developed a structure made of scintillating fibers with an APD (Avalanche PhotoDiode) readout. A dedicated electronics has been developed, and extensive studies have been carried on[13]. This module is used to determine the longitudinal coordinate of impact of the positron on the TC for track reconstruction improvement.

3. Beautiful, but will it work?

A vital issue is to insure the stability of detector performances during all data taking period, which is planned to extend over two years or more. Thus several calibration techniques have been implemented.

The most delicate issue is the LXe calorimeter energy resolution. This depends heavily on the charge and conversion depth reconstruction; lastly, the key parameters are:

- the PMT gain and Quantum Efficiency;

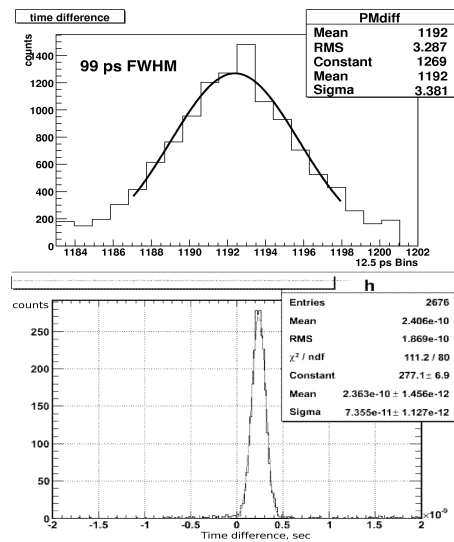


Figure 5. Upper: timing resolution obtained at BTF with a telescope-like configuration, having a well defined impact point. The reported time resolution of 99 ps FWHM for T1-T2 is the value found in one position of a single TC bar, but we obtained a rather uniform resolution within all bars and for a vast set of position for each bar. Lower: time reconstruction in the final configuration obtained with Michel positrons; in this case the timing resolution is degraded by some trajectory spread but still in fair agreement with the required value.

- the Liquid Xenon contamination.

several independent methods each with some advantages and drawbacks are been studied for both of these items. We can distinguish at first from methods that require to stop normal data taking and arrange some apparatus modification, thus being time-consuming, and methods that don't require any tuning nor stopping the normal beam operations, and can thus be performed online.

First we look to "online" calibration and monitoring methods. In this group we can also distinguish between "physical" and "non physical" processes. The easiest one is to feed a light pulse with several LEDs put in various positions on the inner surface of the LXe vessel. By monitoring with different pulse height and looking for the PMT response one can observe variation in the PMT gain. Another alternative method, which is addressed mainly to timing accuracy, involves the use of a very fast laser pulse (10 ps total width) with a wavelength close to the characteristic emission of the Xe; this is fed into the vessel and simultaneously into the TC with a very low dispersion optical fiber and allows to monitor the relative synchronization of the two timing detector. Also, this can help in observing dramatic variation of the TC PMT response, that could affect the whole experiment outcome, for example biasing in unwanted manner the trigger-level event selection. A third method is a physical one and relies on several α sources immersed in LXe[14]. Each source is a small deposition of ^{241}Am on a 100 μm diameter gold plated tungsten wire. Half life of americium is suitable to have a uniform activity during all data taking. Having a well-defined energy deposit into LXe, it is possible with this method to estimate PMT QE and the monitor optical properties of LXe that are affected by the eventual presence of very small amounts of contaminants[4], as shown in fig. 6.

A last way is the use of normal Radiative Decay of muons stopped on target. This result in a looser time and direction correlation between positron and gamma, and also both of them has lower energies, but this can be useful also for normalizing purposes as well as for testing event

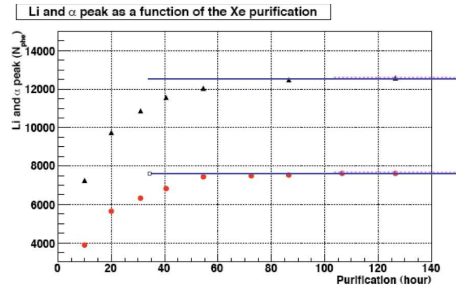


Figure 6. Example of monitoring the LXe purification with α sources and $\text{Li}(p\gamma)\text{Be}$ methods. It is evident the plateau in the detector response reached after ≈ 80 hours of purification progress.

reconstruction capability. A dedicated tool for DCs is the naive Michel trigger, helping in characterizing their ability to track positrons trajectories back to the target; to allow this, the target presents some "holes" that can be reconstructed and can give an estimate on the resolution of vertex reconstruction.

Concerning the "offline" methods, we have two physical handles to test detector performances:

- a CW accelerator providing mono-energetic low energy photons;
- a π^+ beam for production of high energy photons.

The first item relies on the production of low energy photons by means of nuclear reactions of the type $X(p, \gamma)Y$ where X and Y are two contiguous low- Z elements, and the proton can have up to 1 MeV energy [15,16]. Photons are emitted by the higher Z elements being generated, by means of nuclear de-excitation. Main candidates are the reactions involving Boron and Lithium as target materials, undergoing the reactions $B(p, \gamma)C$ and $Li(p, \gamma)Be$. The boron reaction has a resonance at around 870 keV and the result is the emission of either a single 16.1 MeV photon or a couple of mono-energetic (11.4 and 4.7 MeV respectively) photons. The double photon

emission proved to be useful to look up for TC-Xe synchronizing. On the other side the Lithium target provides a nice 17.6 MeV photon, via the xxx keV-resonant proton reaction. To obtain protons with the needed energies, a Cockcroft-Walton accelerator with a dedicated beam line entering the COBRA magnet has been implemented; it can reach energies up to 1 MeV, suitable for our purposes.

A set of Boron and Lithium Fluoride targets have been produced in the Genova film deposition facility[11]. The "Boron Way" has some advantages: the CW beam line can be easily inserted into the COBRA magnet in a few minutes, and within a reasonable live time a sufficient statistics is reached for calibration and monitoring measurements. Thus it can be used quite often, for instance during the periodical shutdown of the PSI main accelerator, when muon beam is not available.

The last method relies on the charge exchange reaction $\pi^+ + n \rightarrow \pi_0 + p$ [4], where the final π_0 decays into two photons being at rest in the lab frame. According to the kinematics of the process this will result in a couple of photons of energies 55 and 83 MeV respectively, emitted back-to-back. They are detected with the coincidence of the LXe signal with a reference NaI thus eliminating not back-to-back events which will result in a wider energy distribution. By measuring the line width for the 55 MeV line one can monitor the LXe calorimeter energy resolution, while comparing $t_{Xe} - t_{NaI}$ an estimate of timing resolution is obtained; both issues are reported in figure 2. The main drawback of this method is that one have to change the beam line parameters to extract pions instead of muons and the best suited target for the charge exchange reaction is a liquid hydrogen target that needs several days to be installed. Thus this method will be used in the very beginning of data taking to validate the detector performances.

4. Final detector performances and experiment goals

In summer 2008 MEG data taking is started.

Table 1
MEG performances and expected goal, to be obtained within 2008 beam time

Detector performances	Obtained
Muon Stopping Rate	$3 \cdot 10^7 \mu/s$
DC momentum resolution	1.1 %
DC vertex reconstruction	± 3 mm
$e^+ - \gamma$ angular resolution	± 17 mrad
TC timing resolution	120 ps FWHM
LXe energy resolution	5% FWHM
LXe timing resolution	150 ps FWHM
LXe efficiency	$\pm 40\%$
Experimental goals	Planned
Single Event Sens.	2.2×10^{-13}
Accidental rate	$< 10^{-13}$
90% CL limit	6.9×10^{-13}

Final performances of various detectors are summarized in table 1, where MEG goal is also reported. A very preliminary result from the 2007 Engineering Run can be estimated as an upper limit of about 1.5×10^{-10} [17] which is already within one order of magnitude from the MEGA limit; moreover, many improvements have been implemented in the detector performances and others are planned, that together with the higher statistic from the next weeks of beam time will result in a much lower limit, at least one order of magnitude better than the previous one.

The MEG experiment is planned to take data until 2010, with an intermediate stop due to beam-sharing with other experiments, which will be used for detector and DAQ improvements.

REFERENCES

1. A. Baldini, [MEG Collaboration], at http://meg.psi.ch/docs/prop_infn/nproposal.ps.
2. M. Ahmed *et al.*, Phys. Rev. D 65 (2002) 112002, arXiv:hep-ex/0111030.
3. S. Dussoni, PhD thesis, May 2006, University of Genova, at http://meg.psi.ch/docs/theses/dussoni_phd.pdf.
4. G. Signorelli, PhD thesis, February 2005, Scuola Normale Superiore di Pisa, at meg.psi.ch/docs/theses/tesi_signorelli.pdf.

5. R. Barbieri et al., Nucl. Phys. B445 (1995) 215.
J. Hisano et al., Phys. Rev. B391 (1997) 341.
R. Ciafaloni et al., Nucl. Phys. B458 (1996) 254.
K. S. Babu, J. C. Pati, P. Rastogi, Phys.Lett. B621 (2005) 160-170; arXiv:hep-ph/0502152.
V. Cirigliano, B. Grinstein, G. Isidori, M. B. Wise, Nucl.Phys. B728 (2005) 121, arXiv:hep-ph/0507001.
6. K. Ozone, PhD thesis, March 2005, University of Tokyo, at meg.web.psi.ch/docs/theses/ozoned.pdf.
7. A. Baldini *et al.*, IEEE Trans.Dielectr.Electr.Insul. 13 (2006) 547, arXiv:physics/0401072.
8. T. Doke and K. Masuda, Nucl. Instr. Meth. A420 (1999) 62
C. Rubbia, CERN EP Internal Report 77-8 (1977)
E. Conti *et al.* [EXO Collaboration], Phys. Rev. B 68 (2003) 054201. arXiv:hep-ex/0303008.
9. E. Morikawa *et al.*, J. Chem. Phys. 91 (1989) 1469.
P. Belli *et al.* Nucl. Instr. Meth. **A310** (1991) 150.
A. S. Schlüsser *et al.*, Appl. Phys. Lett. **77** (2000) 1.
10. <http://www.hamamatsu.com>
11. R. Valle, PhD thesis, May 2006, University of Genova, at meg.web.psi.ch/docs/theses/valle_phd.pdf.
12. <http://www.saint-gobain.com>
13. "Development and characterization of scintillating fiber-APD based detector." M. De Gerone, poster presented at NDIP 2008, to be published.
14. A. Baldini *et al.*, MEG Technical Note 29, available at <https://midas.psi.ch/elogs/Technical+Notes/26>.
15. A. Baldini *et al.*, MEG Technical Note 43, available at <https://midas.psi.ch/elogs/Technical+Notes/41>.
16. A. Baldini *et al.*, MEG Technical Note 32, available at <https://midas.psi.ch/elogs/Technical+Notes/29>.
17. W. Ootani, presented at the 2008 collab-

oration seminar "Lepton Flavor Violation with most intense muon beam", University of Tokyo, 2008 (unpublished).